Using Multiple Isotopes to Identify Sources and Transports of Nitrate in Urban Residential Stormwater Runoff

Qiyue Hu
Zhejiang University of Technology
Song Zhu
Zhejiang Construction Investment Environment Engineering
Zanfang Jin (jinzanfang@zjut.edu.cn)
Zhejiang University of Technology https://orcid.org/0000-0002-5529-0899
Aijing Wu
Zhejiang University of Technology
Xiaoyu Chen
Zhejiang University of Technology
Feili Li
Zhejiang University of Technology

Research Article

Keywords: Roof runoff, Road runoff, Nitrogen, Nitrate, Stable isotopes, SIAR model, Urban Residential area

Posted Date: June 22nd, 2021

DOI: https://doi.org/10.21203/rs.3.rs-559827/v1

Highlights

- High levels of DON, PN and NO_3^- in road runoff caused more TN in urban road runoff.
- Atmospheric deposition was the predominant NO_3^- source in urban roof runoff.
- 88-98% of NO_3^- from atmospheric deposition and fertilisers in urban road runoff.
- Soil and organic N had little contribution to NO_3^- both in roof and road runoff.
- NO_3^- from fertilisers was derived from green land in urban residential area.

Using Multiple Isotopes to Identify Sources and Transport of Nitrate in Urban Residential Stormwater Runoff

Qiyue Hu[a], Song Zhu[b], Jin Zanfang[a], Aijing Wu[a], Xiaoyu Chen[a], Feili Li[a]

[a]College of Environment, Zhejiang University of Technology, Hangzhou 310032, China

[b]Zhejiang Construction Investment Environment Engineering Co., Ltd., Hangzhou 31000, China

Corresponding author: Zanfang Jin

1. Zanfang Jin

E-mail: jinzanfang@zjut.edu.cn

Full postal address: College of Environment, Zhejiang University of Technology, Hangzhou 310032, China

Phone: +86-571-88320560

Fax: +86-571-88320560

Abstract: Increased nitrogen (N) from urban stormwater runoff aggravates the deterioration of aquatic ecosystems as urbanisation develops. In this study, the sources and transport of nitrate (NO_3^-) in urban stormwater runoff were investigated by analysing different forms of N, water isotopes ($\delta D\text{-}H_2O$ and $\delta^{18}O\text{-}H_2O$), and NO_3^- isotopes ($\delta^{15}N\text{-}NO_3^-$ and $\delta^{18}O\text{-}NO_3^-$) in urban stormwater runoff in a residential area in Hangzhou, China. The results showed that the concentrations of total N and nitrate N in road runoff were higher than those in roof runoff. Moreover, high concentrations of dissolved organic N and particulate N in road runoff led to significantly different TN concentrations in road runoff (mean: 3.76 mg/L) and roof runoff (mean: 1.23 mg/L). The high $\delta^{18}O\text{-}NO_3^-$ values (mean: 60±13.1‰) indicated that atmospheric deposition was the predominant NO_3^- source in roof runoff, as confirmed by the Bayesian isotope mixing model (SIAR model), contributing 83.6–97.8% to NO_3^-. The SIAR model results demonstrated that atmospheric deposition (34.2–91.9%) and chemical fertilisers (6.27–54.3%) were the main NO_3^- sources for the road runoff. The proportional contributions from soil and organic N were smaller than other sources in both the road runoff and roof runoff. For the initial period, the NO_3^- contributions from atmospheric deposition and chemical fertilisers were higher and lower, respectively, than those in the middle and late periods in road runoff during storm events 3 and 4, while an opposite trend of road runoff in storm event 7 highlighted the influence of short antecedent dry weather period. It was suggested that reducing impervious areas and more effective management of fertiliser application in urban green land areas were essential to minimize the presence of N in urban aquatic

ecosystems.

Keywords: Roof runoff, Road runoff, Nitrogen, Nitrate, Stable isotopes, SIAR model, Urban Residential area

1. Introduction

Increasing urbanisation worldwide has led to population explosion and changes in land use. Owing to the replacement of vegetation and permeable soil by impervious cover, a considerable amount of concrete floor constructed in urban areas causes stormwater runoff to easily collect pollutants (Al Mamoon et al., 2019; Muller et al., 2020; Silva and da Silva 2020; Kolasa-Wiecek and Suszanowicz 2021). Urban stormwater runoff containing large quantities of contaminants, such as organic matter, phosphorus, and N, is considered to be an important pathway for the delivery of contaminants to urban aquatic ecosystems (Li et al., 2016; Al Mamoon et al., 2019). Studies have investigated stormwater runoff pollution from impervious surfaces since the 1980s (Myers et al., 1982; Gromaire-Mertz et al., 1999; Kim et al., 2007; Ballo et al., 2009; Chow and Yusop 2014; Wu et al., 2015; Yang and Toor 2016). Yan et al., (2019) indicated that stormwater runoff was regarded as the largest source of total nitrogen (TN), chemical oxygen demand (COD), and ammonium nitrogen (NH_4^+-N) in the Taihu Basin, China. Silva et al., (2019) demonstrated that increasing impervious areas in the catchment enhanced the nutrient inputs from stormwater runoff, carrying total suspended solids (TSS), total phosphorus, and nitrate (NO_3^-) into Lake Pampulha, Brazil at the beginning of the wet season.

Nitrogen pollution loads account for a large proportion of pollution in urban stormwater and contribute to the degradation of urban water quality, especially owing to algal blooms and eutrophication (Carey et al., 2013; Yang et al., 2020). For example, it was reported that stormwater from impervious surfaces contributed 80% of dissolved N to urban rivers in Melbourne, Australia, contributing to the risk of water eutrophication (Taylor et al., 2005). Further, in recent years, eutrophication in urban aquatic ecosystems has hindered the sustainable development of cities in China (Li et al., 2019a). Therefore, it is important to identify N sources and to study their transport to minimise the transport of N by urban stormwater runoff to urban aquatic ecosystems.

Stable N and oxygen isotopes of NO_3^- ($\delta^{15}N\text{-}NO_3^-$ and $\delta^{18}O\text{-}NO_3^-$) have been widely used to identify NO_3^- sources and reveal N transport and transformation in aquatic ecosystems (Spoelstra et al., 2001; Kendall et al., 2007; Kojima et al., 2011; Rose et al., 2015; Yue et al., 2020; Liu et al., 2021). In recent years, with the development of technology, the content of N and oxygen isotopes combined with a Bayesian isotope mixing model (SIAR model) has been successfully applied to clarify the proportions of different N sources in urban runoff (Yang and Toor 2016; Yang and Toor 2017; Baral et al., 2018; Jani et al., 2020). Hale et al., (2014) investigated the values of $\delta^{15}N\text{-}NO_3^-$ and $\delta^{18}O\text{-}NO_3^-$ in urban watersheds in Central Arizona and identified that fertiliser was the major source of NO_3^- in stormwater runoff, accounting for 38–50% of the NO_3^- load. It was found that the $\delta^{15}N$ values ranged from -11.5‰ to 4.9‰ and that atmospheric deposition (43–71%) and chemical

fertilisers (<1–49%) were the dominant NO_3^- sources in urban residential stormwater runoff in Florida (Yang and Toor 2016).

Residential areas have relatively frequent human activity within cities. In recent years, urban residential areas have been increasingly constructed due to the boom in the real estate industry in China, leading to an increase of impervious surfaces within residential areas, and accordingly, an increase in stormwater runoff carrying pollutants directly into urban rivers (Li et al., 2019b; Wen et al., 2019; Liu et al., 2020). Compared to China, more researches on stormwater runoff in residential areas have been conducted in other countries, whereas researches on stormwater runoff in China have focused more on non-point source pollution in agricultural areas (Sui et al., 2020). In residential areas, impervious surfaces mainly comprise roads and roofs, and the different types of human activities on roads and roofs lead to the corresponding differences in characteristic pollutants (Yang and Toor 2017). For instance, Kojima et al., (2011) demonstrated that N in road dust mainly originated from fertilisers and soil, while the N source in roof dust originated from atmospheric deposition.

In this study, stormwater runoff was collected from roads and roofs in an urban residential area, and the concentration of different forms of N and stable isotopes of NO_3^- ($\delta^{15}N\text{-}NO_3^-$ and $\delta^{18}O\text{-}NO_3^-$) were measured. The objectives were to evaluate the spatial and temporal distributions of the different forms of N and to quantify the major N sources in urban residential stormwater runoff. This study serves as a guideline for generating more effective mitigation strategies to reduce the concentration of N in urban aquatic ecosystems.

2. Materials and methods

2.1 Study site

The residential study area (30°17′N, 120°9′E) is located in Hangzhou, which is the political, economic, and cultural center of Zhejiang Province, East China (Fig. 1). The continuously growing population in Hangzhou has increased from 889.2 million in 2014 to 1036 million in 2019, and the urbanization rate of Hangzhou reached 78.5% in 2019 (HZSB 2020). The residential area comprises approximately 12.7 ha, of which green land accounts for 27% and the rest are impervious surfaces (rooftops: 36%, driveways and sidewalks: 17%, and roads: 20%) is 73%. The age of construction in the study area is more than 30 years with 2525 households, and the area is served by a separate sewer system. We collected the roof runoff at the top of a five-storey residential building (approximately 15 m in height) which featured an open-area cement roof without any shelter. Road runoff was collected on a residential road of bituminous concrete which featured tree, grass, and other plants planted on both sides of the roads. The overall study region is characterised by a subtropical monsoon climate with an annual average temperature of 15.7 ℃ and annual average rainfall of 1454 mm, of which 67% occurs during the wet season (March–September). The average annual rainfall was 1584.7 mm from 2019 to 2020, and monthly rainfall ranged from 37.7 to 374.7 mm in the wet season in Hangzhou (HZSB 2020). The study period was from March to August.

2.2 Sampling and analysis

A weather application showing the evolution of storm events was used to track storm events in the study area. Stormwater runoff samples were collected manually after identifying a major storm event. An acid-washed polyethylene container was used to gather runoff samples before the runoff flowed into the rain drainage systems. The roof and road runoff were collected at the top of the five-storey residential building (Site A) and on the road in the residential area (Site B), respectively (Fig. 1). At each catchment site, samples were collected at 5 minutes intervals within 1.5–2 h during each storm and were placed in a 500 mL plastic bottle. The stormwater runoff samples were collected during seven storm events, leading to a total of 321 samples (165 roof and 156 road runoff samples) (Fig. 1). After sampling, a portion of the samples was filtered through 0.45 μm membrane filters (Whatman) into 100 mL acid-washed polyethylene bottles on the sampling day and stored in a refrigerator at -20 ℃ until the analysis of dissolved total nitrogen (DTN), major ions (NH_4^+, NO_2^- and NO_3^-) and isotopes. The other portion was not filtered and stored at -4 ℃ for TN and COD analysis within 48 h.

TN and DTN were measured using the alkaline potassium persulfate digestion ultraviolet spectrophotometric method (HJ636-2012). Total suspended solids and COD were analysed using the gravimetric method (GB11901-89) and the fast digestion-spectrophotometric method (HJ/T399-2007), respectively. The concentrations of NH_4^+, NO_2^-, and NO_3^- were measured using ion chromatography (Dionex ICS-900). The NO_2^- concentrations in most of the samples were below the

detection limit (BDL); therefore, dissolved inorganic nitrogen (DIN) was defined as the sum of NH_4^+-N and nitrate nitrogen (NO_3^--N). The dissolved organic nitrogen (DON) and particulate nitrogen (PN) were calculated using the following mass balance: [DON] = [DTN] - [DIN] and [PN] = [TN] - [DTN].

Twenty-two road runoff samples were analysed for hydrogen and oxygen isotopes of water (δD-H_2O and δ^{18}O-H_2O) using an isotopic water analyser (Picarro L2140-i). The precisions of δD-H_2O and δ^{18}O-H_2O were ±0.5‰ and ±0.1‰, respectively. Thirty-two roof runoff and thirty-five surface runoff samples were analysed for stable N and oxygen isotopes of NO_3^- (δ^{15}N-NO_3^- and δ^{18}O-NO_3^-) which were evaluated according to the bacterial denitrification method (Kaiser et al., 2007; McIlvin and Casciotti 2011). In brief, denitrifying bacteria (*Pseudomonas aureofaciens*) lacking gaseous nitrous oxide (N_2O), converted NO_3^- from the water samples to N_2O through reductase activity. Then, the N_2O was stripped from the vial by helium carrier gas, purified using cryogenic trapping, and analysed by isotope ratio mass spectrometry (Thermo scientific DELTA V Advantage). The analytical errors for δ^{15}N-NO_3^- and δ^{18}O-NO_3^- were ±0.3‰ and ±0.5‰, respectively. In this paper, isotopic results are expressed as δ values (per mil unit), such that

$$\delta(‰)=1000\times\left(\frac{R_{sample}}{R_{standard}}-1\right),$$

where R is the isotopic rate (^{15}N/^{14}N, ^{18}O/^{16}O, and D/H). The standard of ^{15}N/^{14}N was atmospheric air (AIR), and the collective standard of ^{18}O/^{16}O and D/H was the Vienna Standard Mean Ocean Water (VSMOW).

2.3 SIAR model

The proportions of the different NO_3^- source contributions were evaluated by the SIAR model. The SIAR model can be expressed as follows (Parnell et al., 2010):

$$X_{ij} = \sum_{k=1}^{K} p_k\left(S_{jk} + C_{jk}\right) + \varepsilon_{ij};$$

$$S_{ij} \sim N\left(\mu_{jk}, \omega_{jk}^2\right);$$

$$C_{jk} \sim N\left(\lambda_{jk}, \tau_{jk}^2\right);$$

$$\varepsilon_{jk} \sim N\left(0, \sigma_j^2\right);$$

where X_{ij} is the isotope value j of the mixture i (i=1, 2, 3,..., N, and j=1, 2, 3,..., J); S_{jk} is the isotope value j in source k (k=1, 2, 3,..., K), which conforms to a normal distribution with a mean of μ_{jk} and a standard variance of ω_{jk}^2; C_{jk} is the fractionation coefficient for isotope j for source k, which is a standard distribution with a mean value of λ_{jk} and a variance of τ_{jk}^2; and ε_{ij} is the residual error, which is used to characterise the remaining unquantified variation between the individual mixed samples and is a normal distribution with a mean value of 0 and a variance of σ_j^2. The variable p_k is the proportional contribution of source k, estimated using the SIAR model.

3. Results and discussion

3.1 N concentration and N forms in stormwater runoff

The concentrations of TN, DTN, NH_4^+-N, NO_3^--N, PN and DON in roof runoff and road runoff for 2019–2020 are shown in Table 2. The concentrations of TN, NH_4^+-N,

and NO_3^--N in the roof runoff of seven storm events ranged from 0.26–6.13 (mean 1.23 mg/L), 0.03–1.96 (mean 0.42 mg/L), BDL–1.69 (mean 0.26 mg/L), respectively. The concentrations of TN, NH_4^+-N, and NO_3^--N in the road runoff of the same seven storm events were higher than those in the roof runoff (TN: 0.65–12.7 (mean 3.76 mg/L), NH_4^+-N: BDL–5.28 (mean 0.50 mg/L), and NO_3^--N: BDL–3.05 (mean 0.50 mg/L)). The concentrations of PN and DON in roof and road runoff also showed the same trend as those of TN, NH_4^+-N, and NO_3^--N. In addition, the concentrations of TN, PN, and DON in road runoff were more than three times higher than as those in the roof runoff in the same storm event, proving the important influence of surrounding land use on N in stormwater runoff (Table 2). Road runoff is an important source of nonpoint pollution in urban aquatic ecosystems because the N compounds within the road dust, chemical fertiliser, soil materials, pet waste, and leaf litter on road surfaces are eventually washed into stormwater runoff (Lusk and Toor 2016; Janke et al., 2017; Yang and Toor 2017). In contrast, human activities had relatively little impact on the roof runoff, while atmospheric deposition and organic N, such as bird and rodent droppings, were the main N sources on the cement roof surfaces (Song et al., 2019). Moreover, the TN concentration was dominated by PN and DON in road runoff, while NH_4^+-N and NO_3^--N were the major N compounds in roof runoff (Table 2). The results were consistent with those of Vaze and Chiew (2004), who found that the proportion of DTN in TN ranged between 20% and 50%, and proportion of PN in TN ranged from 50% to 80% in road runoff in Australia. It was suggested that roads were more likely to accumulate particulate matter than roofs, and

237 that the particulate matter in the soil on the sides of the roads was easily mobilised
238 and transported to the impervious surface through stormwater runoff. Previous studies
239 have also documented that climatic such as the frequency and intensity of storms and
240 antecedent rainfall conditions have significant impacts on the concentrations of N in
241 stormwater runoff, leading to a wide range of N concentrations in stormwater runoff
242 (Yang and Lusk 2018). The mean concentration of TN in road runoff in this study
243 (3.76 mg/L) was higher than that in road runoff in humid subtropical urban residential
244 areas in Tampa, Florida, (TN: 0.42 mg/L) and much lower than that in a study
245 conducted on road runoff in a semi-arid urban residential area in the Aliso Creek
246 watershed, California (TN: 10.85 mg/L) (Toor et al., 2017; Yang and Toor 2017).
247 Significantly positive correlations ($P<0.01$) were found between antecedent dry
248 weather period and TN, DTN, NH_4^+-N, and DON concentrations, both in roof runoff
249 and road runoff, revealing that N concentrations in stormwater runoff are linked to the
250 duration of dry periods before storm events (Table S1). Lewis and Grimm (2007) also
251 reported high NH_4^+-N concentration in stormwater runoff in arid urban catchments
252 after a longer antecedent dry period. Higher concentrations of TN, DTN, NH_4^+-N, and
253 DON were observed in roof and road runoff during storm event 2, as compared to
254 those in other storm events. This is attributed to the longer antecedent dry weather
255 period (13 days) preceding 13 May 2019. As pollutants accumulate on impervious
256 surfaces during antecedent dry periods, the stormwater runoff after a longer
257 antecedent dry weather period carries more pollutants (Lewis and Grimm 2007; Li et
258 al., 2007a; Zhi et al., 2018). The PN and DON concentrations in the road runoff were

higher in May than those in the other months (Table 2). Furthermore, higher concentrations of PN corresponded to the higher concentrations of TSS in road runoff (Table 2). Similarly, higher concentrations of DON were consistent with the higher concentrations of COD in road runoff (Table 2). Significantly positive correlations ($P<0.01$) were found between TSS and PN, COD, and DON concentrations, in road runoff (Table S1). This may be attributed to extensive plant growth during May, which is a warm and humid month in late spring. During this time, organic matter, including leaf litter, flower debris, pollen, and seeds, are expected to reach the ground and eventually enter into stormwater runoff, increasing the organic N load of the road runoff in the urban residential area. These results are in agreement with Janke et al., (2017), who found that seasonal peaks of N in urban stormwater runoff coincided with spring leaf-out and flowering.

The mean concentrations of NO_3^--N were lower than the mean concentrations of NH_4^+-N in roof runoff, while the opposite was true for in road runoff (Table 2). NO_3^--N concentrations were lower than NH_4^+-N concentrations, and the mean NO_3^--N/NH_4^+-N ratio was found to be 0.87 in rainwater of Hangzhou from 2015 to 2017 (Jin et al., 2019). In this study, all mean NO_3^--N/NH_4^+-N ratios in the roof runoff of the seven storm events were lower than 1.0, indicating that atmospheric deposition was the dominant N source in the roof runoff. The NO_3^--N/NH_4^+-N ratios in road runoff varied widely (0.37–2.33). In addition to atmospheric deposition, it was found that anthropogenic inputs, such as chemical fertilisers, soil materials, pet waste, and leaf litter, also influenced the NO_3^--N and NH_4^+-N concentrations in road runoff.

281 NO_3^--N may have been preferentially washed out from surface deposits, and NH_4^+-N
282 could have been easily absorbed by surface deposits (Kojima et al., 2011; Wang et al.,
283 2019). However, the NO_3^--N/NH_4^+-N ratios in road runoff in May (storm events 2 and
284 5) were much lower than those in other months (Table 2). On the one hand, due to the
285 increased air temperature and humidity in May, the activities of microbes were likely
286 enhanced; therefore, the mineralisation of tree branches, leaf litter, flower debris, and
287 soil organic N was likely a significant contributor to the NH_4^+-N in road runoff. On
288 the other hand, low rainfall in May would not have been conducive to NO_3^--N export
289 in stormwater runoff (Kaushal et al., 2014). The above two reasons could explain why
290 the NO_3^--N concentrations were lower and the NH_4^+-N concentrations were higher in
291 road runoff in May than in other months.

292 The temporal variation of N forms in roof and road runoff during the seven storm
293 events is shown in Fig. S1. The concentrations of TN, NH_4^+-N, and NO_3^--N in roof
294 and road runoff were higher in the beginning of the storm event, and then gradually
295 stabilized with an increase in rainfall duration. Climate variables such as the
296 frequency and intensity of storms are important factors that influence N transport in
297 stormwater runoff, and NO_3^--N exports in stormwater runoff increased during strong
298 storms (Kaushal et al., 2014; Li et al., 2015). For example, the comprehensive wind
299 and rain intensity index of Super Typhoon Lekima was 158.6, and the rainfall amount
300 during the sampling period was 19.1 mm on 9 August 2019 (NMC, 2019). The onrush
301 of water that accompanied strong winds during Super Typhoon Lekima caused a
302 strong scouring effect on the land. As a result, the temporal variations in NO_3^--N

concentrations in the road runoff of storm event 4 (9 August 2019) showed significant fluctuations. Owing to the low rainfall, the temporal variations of NO_3^--N concentrations in road runoff during storm events 2 and 5 were maintained at a low level. The antecedent conditions could have also affected N transport in the stormwater runoff (Lee et al., 2002; Taebi and Droste 2004). Thus, it is considered that the temporal variations of TN, NO_3^--N, and NH_4^+-N concentrations in the roof runoff of event 7 were more stable owing to a lower rainfall amount and relatively short antecedent dry weather period.

3.2 Water sources of stormwater runoff

Unlike roof runoff, road runoff can originate from a combination of various water sources, such as rainfall and municipal water in urban residential areas. Therefore, water isotopes were used to identify the water sources in the road runoff. The values of δD-H_2O ranged from -72.2‰ to -26.1‰ (mean -52.5‰) and the δ^{18}O-H_2O values ranged from -10.5‰ to -4.3‰ (mean -7.7‰) in road runoff (n=22) (Fig.2 and Table S1). The relationship between δ^{18}O-H_2O and δD-H_2O in road runoff could be explained as δD-H_2O=7.6 δ^{18}O-H_2O+6.2 (R^2=0.99), which was closely correlated with the global meteoric water line (GMWL) interpreted as δD-H_2O=8 δ^{18}O-H_2O+10 (Craig 1961). The y-intercept (deuterium excess), which is explained by the equation *d*-excess=δD-H_2O-8δ^{18}O-H_2O, is a useful tool for evaluating the contribution of evaporated moisture (Gat et al., 1994). The *d*-excess of the road runoff (mean: 9.4‰) was slightly lower than the GMWL (10‰), suggesting that slight evaporation

occurred during runoff generation. Owing to the high temperature during the study period and the impervious surface in the study area (73%), evaporation was likely to take place as runoff travelled over the impervious surface. The relationship between the $\delta^{18}O\text{-}H_2O$ and $\delta D\text{-}H_2O$ values of road runoff therefore suggested that road runoff during storms originated from local rainwater with little evaporation and not from other water sources such as reclaimed water, municipal water, or leaking sanitary sewers.

3.3 NO_3^- sources in stormwater runoff

3.3.1 Identifying NO_3^- sources and NO_3^- transport in stormwater runoff

The $\delta^{18}O\text{-}NO_3^-$ values varied from 39.9‰ to 79.8‰ (mean: 60±13.1‰) in roof runoff, and from 15.6‰ to 74.3‰ (mean: 40.6±21.7‰) in road runoff (Fig.3 and Table S2). Temporal variations of $\delta^{18}O\text{-}NO_3^-$ in stormwater runoff during storm events 3, 4, and 7 were shown in Fig. 4. The temporal variations of $\delta^{18}O\text{-}NO_3^-$ in roof runoff were not obvious, and the $\delta^{18}O\text{-}NO_3^-$ values in the roof runoff remained at a high level. The $\delta^{18}O\text{-}NO_3^-$ values of rainwater and dry deposition in Hangzhou in wet season were 31.5–71.6‰ (mean: 57.4‰), and 24.5–79.2‰ (mean: 62.5‰), respectively ((Jin et al., 2019; Jin et al., 2021). The high $\delta^{18}O\text{-}NO_3^-$ values in roof runoff were similar to the $\delta^{18}O\text{-}NO_3^-$ values of rainwater and dry deposition, implying that the atmospheric deposition (both dry and wet) was the dominant NO_3^--N source in roof runoff (Fig. 3). Thus, the higher values of $\delta^{18}O\text{-}NO_3^-$ in roof and road runoff for storm event 7 than those in other events resulted from the influence of the high $\delta^{18}O\text{-}NO_3^-$ values of

atmospheric deposition (Fig. 4). The $\delta^{18}O\text{-}NO_3^-$ values in road runoff were lower than those in roof runoff, and were further from the $\delta^{18}O\text{-}NO_3^-$ values in rainwater and dry deposits in Hangzhou, indicating that NO_3^--N from other sources was carried with the urban stormwater runoff.

The $\delta^{15}N\text{-}NO_3^-$ values ranged from -10.7‰ to 1.4‰ (mean: -4.0±3.3‰) in roof runoff, and from -8.6‰ to 8.4‰ (mean: -2.9±3.1‰) in road runoff (Fig. 3 and Table S2). The $\delta^{15}N\text{-}NO_3^-$ values of rainwater (-4.4‰ to 3.6‰) and dry deposition (-1.0‰ to 5.8‰) in Hangzhou during the wet season were in the range of the $\delta^{15}N\text{-}NO_3^-$ values in road runoff, suggesting that other NO_3^- sources contributed to road runoff in addition to the atmospheric NO_3^- (Fig. 3) (Jin et al., 2019; Jin et al., 2021). The $\delta^{15}N\text{-}NO_3^-$ values in roof and road runoff in the urban residential area in Hangzhou were higher than the $\delta^{15}N\text{-}NO_3^-$ values in forest runoff (mean: -6.07‰) reported by Zhang et al., (2019) because chemical fertilisers with low $\delta^{15}N\text{-}NO_3^-$ values were identified as the main NO_3^- source in forest runoff. The $\delta^{15}N\text{-}NO_3^-$ and $\delta^{18}O\text{-}NO_3^-$ values of roof and road runoff portrayed in Fig. 3 demonstrate that atmospheric deposition was the only NO_3^- source in roof runoff, while NO_3^- sources of road runoff mainly reflected a mixture of atmospheric deposition and chemical fertilisers during the study period. Previous studies have pointed out that chemical fertilisers contributed an average of 16–64% of NO_3^--N in road runoff, and a large proportion of N inputs were from chemical fertilisers application for residential lawns and plants in urban residential areas (Riha et al., 2014; Yang and Toor 2017; Muller et al., 2020). The estimated annual NPK (nitrogen–phosphorus–potassium) compound fertiliser

367 application (containing NO_3^- fertiliser and NH_4^+ fertiliser)in urban green land was
368 found to be 75–150 kg N/ha (two applications on average) in Hangzhou (Teaching
369 Material Office of the Ministry of Labor and Social Security 2005). Further research
370 has suggested that NO_3^- derived from chemical fertilisers (NO_3^- and NH_4^+ fertiliser)
371 had typical $\delta^{15}N\text{-}NO_3^-$ values from -6‰ to 6‰, and the $\delta^{18}O\text{-}NO_3^-$ values in NH_4^+
372 fertiliser and in NO_3^- fertiliser were from -10 to 10‰ and 17–25‰, respectively
373 (Bateman and Kelly 2007; Xue et al., 2009). Therefore, chemical fertilisers were one
374 of the main NO_3^- sources, as the green coverage rate (27%) in the study area was high.
375 The temporal variations of $\delta^{15}N\text{-}NO_3^-$ values in road runoff in the urban residential
376 area in Hangzhou showed an obvious decrease, whereas the temporal variations of
377 $\delta^{15}N\text{-}NO_3^-$ in roof runoff fluctuated up and down smoothly (Fig. 4). It was implied
378 that NO_3^- sources in road runoff were more varied, which were not only derived from
379 atmospheric deposition but also from chemical fertilisers, soil particles containing N,
380 and organic N sources (pet waste, leaf litter etc.), in comparison with those in roof
381 runoff. Based on the variations of TN and NO_3^- concentrations and the $\delta^{15}N\text{-}NO_3^-$ and
382 $\delta^{18}O\text{-}NO_3^-$ values in stormwater runoff, the first 10 min of the sampling period of each
383 storm event was assumed to be the initial period of stormwater runoff. There are two
384 possible reasons for the high $\delta^{15}N\text{-}NO_3^-$ values in road runoff in the beginning (initial
385 period of stormwater runoff, i.e. the first 10 min of sampling time). First, the elderly
386 population (over 60 years old), accounting for 41.7% of the study area, led to high
387 per-area rates of pet ownership (HZSB 2020); therefore, pets such as dogs that were
388 kept by retired persons may have excreted faeces on roads or green land in residential

areas. For example, dog waste in one urban area of Minnesota has been found to contribute up to 28% of TN inputs (Hobbie et al., 2017). Second, the mineralisation of organic matter including leaf litter, flower debris, pollen, and seeds from trees and other plants on the roadsides, was also a NO_3^- source in stormwater runoff. Similarly, the highest $\delta^{15}N\text{-}NO_3^-$ value of the first sample in roof runoff was also ascribed to organic N (bird and rodent droppings) on the roof surface during storm events 4 and 7. After the surface pollutants were washed away, the soil moisture gradually become saturated. Then, nitrified soil and chemical fertilisers were washed into the road runoff as a result of continuous rainstorms. Thus, low $\delta^{15}N\text{-}NO_3^-$ values in road runoff were observed in the middle and late period of stormwater runoff (i.e. after the first 10 min of sampling time). As reported by Baral et al., (2018), the NO_3^- in stormwater runoff during smaller storms mainly originates from atmospheric deposition. In contrast, the NO_3^- contribution from atmospheric deposition may be lower than that from nitrified soil and fertiliser washed into the stormwater runoff during larger storms. Therefore, in this study, atmospheric deposition is thought to be the main NO_3^- source in road runoff of storm event 7 due to the small rainfall amount and relatively short antecedent dry weather period during the sampling period, which was confirmed by the lower $\delta^{15}N\text{-}NO_3^-$ values and higher $\delta^{18}O\text{-}NO_3^-$ values during storm event 7.

The $\delta^{18}O\text{-}NO_3^-$ values are a useful indicator for identifying whether runoff occurred during nitrification. Nitrate from nitrification has $\delta^{18}O\text{-}NO_3^-$ values from -10‰ to 10‰ (Kendall et al., 2007). Theoretically, the $\delta^{18}O\text{-}NO_3^-$ of nitrification is generated by one

411 oxygen atom from oxygen in the atmosphere, and two oxygen atoms from water. The
412 equation can be expressed as $\delta^{18}O\text{-}NO_3^-=2/3\ (\delta^{18}O\text{-}H_2O)+1/3\ (\delta^{18}O\text{-}O_2)$ (Kendall et
413 al., 2007). According to this equation, it was expected that the theoretical $\delta^{18}O\text{-}NO_3^-$
414 values in the road runoff from nitrification could range from 0.81‰ to 5.00‰. The
415 values of $\delta^{18}O\text{-}H_2O$ and $\delta^{18}O\text{-}NO_3^-$ in the road runoff in storm events 3 and 7
416 demonstrated that NO_3^- contribution from in situ soil nitrification could be ignored
417 (Fig. 5). Generally, denitrification occurs when oxygen is limited and organic carbon
418 is available in an aquatic ecosystem, where bacteria reduce NO_3^- to N_2 or N_2O.
419 Heterotrophic microorganisms metabolise light isotopes (i.e. ^{14}N and ^{16}O) in
420 preference to heavy isotopes (i.e. ^{15}N and ^{18}O) during denitrification (Kendall et al.,
421 2007). Denitrification causes the $\delta^{15}N\text{-}NO_3^-$ and $\delta^{18}O\text{-}NO_3^-$ values of the residual
422 NO_3^- to increase with a $\delta^{15}N\text{-}NO_3^-/\delta^{18}O\text{-}NO_3^-$ ratio from 1:1 to 2:1 (Xue et al., 2009).
423 In this study, no linear relationships between $\delta^{15}N\text{-}NO_3^-$ and $\delta^{18}O\text{-}NO_3^-$ were observed,
424 suggesting that no obvious denitrification occurred in the roof or road runoff in the
425 urban residential area of Hangzhou.

426 **3.3.2 Estimating the contribution of NO_3^- sources**

427 According to the above analysis, two NO_3^- sources (atmospheric deposition and soil
428 and organic N such as bird and rodent droppings) in roof runoff and four NO_3^- sources
429 (atmospheric deposition, NO_3^- fertiliser, NH_4^+ fertiliser, and soil and organic N such
430 as pet waste, leaf litter and soil N) were identified in road runoff in the urban
431 residential area of Hangzhou. The contributions of NO_3^- in the urban residential

stormwater runoff were estimated using the SIAR model. The $\delta^{15}N\text{-}NO_3^-$ and $\delta^{18}O\text{-}NO_3^-$ values of the NO_3^- sources were based on relevant literatures (Bedard-Haughn et al., 2003; Curt et al., 2004; Widory et al., 2004; Kendall et al., 2007; Li et al., 2007b; Divers et al., 2014; Yang and Toor 2016; Jin et al., 2019), as shown in Table S2. We assumed $C_{jk} = 0$ in the SIAR model because of the absence of denitrification in the roof and road runoff in the study area. The contributions of NO_3^- sources to roof and road runoff are shown in Fig. 6 and Table S3. The NO_3^- contributions from atmospheric deposition (83.6–97.8%) was predominant, and the contributions from organic N were only 5.02–16.4% in roof runoff. In road runoff, atmospheric deposition (40.5% in storm event 3; 34.2% in storm event 4) contributed the most, while soil and organic N (6.44% in storm event 3, 11.5% in storm event 4) contributed the least, and NH_4^+ fertiliser (31.3% in storm event 3; 30% in storm event 4) and NO_3^- fertiliser (21.7% in storm event 3; 24.4% in storm event 4) were intermediate. The contribution of atmospheric deposition (91.9%) was dominant, followed by that of NO_3^- fertiliser (3.68%), NH_4^+ fertiliser (2.59%), and soil and organic N (1.82%) in road runoff during storm event 7. In this case, atmospheric deposition was an important contributor to stormwater runoff N in the urban residential area, which is similar to the findings of urban stormwater runoff in Florida, where 30–88% of NO_3^- was found to be from atmospheric deposition (Yang and Toor 2016; Krimsky et al., 2021). Compared with the values in storm events 3 and 4 in this study, a significant increase in the contribution of atmospheric deposition occurred for roof and road runoff during storm event 7, reflecting the short antecedent dry weather

period (1 day). Rain from the previous day would have washed away the N pollutants on the road surface. Accordingly, the NO_3^- contributions in road runoff from chemical fertiliser (NH_4^+ fertiliser and NO_3^- fertiliser), and soil and organic N were relatively low for storm event 7. Our results highlighted that chemical fertiliser (NH_4^+ and NO_3^- fertiliser) were the main NO_3^- source in road runoff (an average contribution of more than 50% in road runoff in storm events 3 and 4), owing to the application of chemical fertilisers for plant growth in urban residential areas. This is in agreement with the investigations in urban areas by Hale et al., (2014) and Krimsky et al., (2021). For example, chemical fertilisers contributed 44% of NO_3^- in stormwater runoff in the urban areas of Phoenix, Arizona (Hale et al., 2014). The NO_3^- contribution from soil and organic N was lower than other NO_3^- sources in road runoff in the urban residential area of Hangzhou. Soil erosion was mitigated by 27% of the green land and 73% of the impervious surface, and road sweeping was carried out on alternate days. Although soil and organic N generally have diverse origins, the quantities of soil particles, leaf litter, and pet waste, etc. that were washed into runoff were likely small.

The SIAR outputs revealed that NO_3^- contributions varied significantly between the initial period and middle and late periods in road runoff during a storm event (Fig. 7 and Table S3). The NO_3^- contributions were similar during the same period in storm events 3 and 4. Atmospheric deposition and chemical fertiliser were the primary N sources in both the initial period and middle and late periods in road runoff in storm events 3 and 4. Coupled with the continuing storm, the combination of atmospheric

476 deposition and chemical fertilisers became more important, suggesting that longer
477 duration storms were more likely to transfer N pollutants from urban green land or
478 urban soils to stormwater runoff. Therefore, we find that during the initial period of
479 stormwater runoff, the storm runoff generated from impervious surfaces was able to
480 quickly wash off the soil, organic matter, and atmospheric dry-deposited NO_3^- on the
481 impervious surface. Thus, the NO_3^- contributions from atmospheric deposition, soil
482 and organic N were higher in the initial period than those in the middle and late
483 periods in road runoff during storm events 3 and 4. Similarly, Lewis and Grimm
484 (2007) revealed that frequent N transport by rain is easier in urban environments. The
485 short antecedent dry weather period (1 day) in storm event 7 was therefore likely
486 responsible for the higher NO_3^- contribution from chemical fertilisers in road runoff
487 during the initial period as compared to the middle and late periods. Moreover, with a
488 decrease in NO_3^- contribution from chemical fertilisers, and soil and organic N, the
489 NO_3^- contribution from atmospheric deposition in road runoff increased dramatically
490 during the middle and late periods for storm event 7.

491 **4 Conclusions**

492 The different forms of N and multiple isotopes ($\delta D\text{-}H_2O$, $\delta^{18}O\text{-}H_2O$, $\delta^{15}N\text{-}NO_3^-$,
493 and $\delta^{18}O\text{-}NO_3^-$) in stormwater runoff were measured from 2019 to 2020 in a typical
494 urban residential area in Hangzhou, East China. The mean concentrations of TN, DTN,
495 PN, DON, NH_4^+-N, and NO_3^--N in road runoff were higher than those in roof runoff.
496 The higher $\delta^{18}O\text{-}NO_3^-$ values in roof runoff revealed that atmospheric deposition was

its dominant NO_3^- source. According to the calculation results of the SIAR model, atmospheric deposition contributed 83.61–97.83% of the NO_3^- in roof runoff. Atmospheric deposition and chemical fertilisers were the major NO_3^- sources in road runoff, with NO_3^- contributions from atmospheric deposition, NH_4^+-N fertiliser and NO_3^--N fertiliser accounted for 34.15–91.91%, 2.59–31.33%, and 3.68–24.35%, respectively. The contributions of soil and organic N to NO_3^- in roof and road runoff were relatively low (1.82-16.39%). The short antecedent dry weather period before storm event 7 had a significant impact on NO_3^- in road runoff, with a dramatically increased contribution of atmospheric deposition to NO_3^-. The results demonstrated that much of the NO_3^- in road runoff originated from impervious areas (soil and organic N) during the initial period of stormwater runoff. Moreover, the NO_3^- contributions from chemical fertilisers increased and those from atmospheric deposition, and soil and organic N decreased in the middle and late periods in road runoff during storm events 3 and 4. However, the short antecedent dry weather period led to a dramatically lower chemical fertiliser contribution to NO_3^- in the middle and late periods in road runoff during storm event 7. The results of this study suggest that it is necessary to take effective measures to optimise chemical fertilisers application and control its loss from urban green land. Frequent road sweeping and cleaning are useful in preventing soil and organic N from entering urban ecosystems. Reducing the amount of impervious areas is also essential to reducing the overall N load in urban ecosystems.

Acknowledgments

The authors gratefully acknowledge the financial support from the National Natural Science Foundation of China (No. 41673097; No. 41373122).

Author's contributions: **Qiyue Hu**: Methodology, Software; Validation; Formal analysis; Investigation; Data curation; Writing - original draft; Writing - review & editing; Visualization. **Song Zhu**: Investigation; Software; Resources. **Zanfang Jin**: Conceptualization; Methodology, Software; Validation; Investigation; Resources; Data curation; Writing - review & editing; Supervision; Project administration; Funding acquisition. **Aijing Wu**: Investigation; Data curation; Visualization. **Xiaoyu Chen**: Investigation. **Feili Li**: Resources.

Funding: This study was supported by the National Natural Science Foundation of China (No. 41673097; No. 41373122).

Data availability: The datasets analyzed during the study are available in the Supplementary Material.

Compliance with ethical standards

Competing interests: The authors declare that they have no competing interests.

Ethics approval: Not applicable

Consent for publication: Not applicable

Consent to participate: Not applicable

References

Al Mamoon A, Jahan S, He X, Joergensen NE, Rahman A (2019) First flush analysis

using a rainfall simulator on a micro catchment in an arid climate. Science of the Total Environment 693: 133552.

Ballo S, Liu M, Hou LJ, Chang J (2009) Pollutants in stormwater runoff in Shanghai (China): Implications for management of urban runoff pollution. Progress In Natural Science-Materials International 19: 873-880.

Baral D, Fisher JR, Florek MJ, Dvorak BI, Snow DD, Admiraal DM (2018) Atmospheric contributions of nitrate to stormwater runoff from two urban watersheds. Journal of Environmental Engineering 144: 05017009.

Bateman A, Kelly S (2007) Fertilizer nitrogen isotope signatures. Isotopes in environmental and health studies 43: 237-247.

Bedard-Haughn A, van Groenigen JW, van Kessel C (2003) Tracing 15N through landscapes: potential uses and precautions. Journal of Hydrology 272: 175-190.

Carey RO, Hochmuth GJ, Martinez CJ, Boyer TH, Dukes MD, Toor GS, Cisar JL (2013) Evaluating nutrient impacts in urban watersheds: Challenges and research opportunities. Environmental Pollution 173: 138-149.

Chow MF, Yusop Z (2014) Characterization and source identification of stormwater runoff in tropical urban catchments. Water Science And Technology 69: 244-252.

Craig HI (1961) Isotopic variations in meteoric waters: Science. Science 133.

Curt M, Aguado PL, Sánchez G, Bigeriego M, Fernández J (2004) Nitrogen isotope ratios of synthetic and organic sources of nitrate water contamination in Spain. Water Air and Soil Pollution 151: 135-142.

Divers MT, Elliott EM, Bain DJ (2014) Quantification of Nitrate Sources to an Urban

561 Stream Using Dual Nitrate Isotopes. Environmental Science & Technology 48:
562 10580-10587.
563 Gat JR, Bowser CJ, Kendall C (1994) The contribution of evaporation from the Great
564 Lakes to the continental atmosphere: estimate based on stable isotope data.
565 Geophysical Research Letters 21: 557-560.
566 GB11901-89. (1990) Water quality–Determination of suspended substance–
567 Gravimetric method. Ministry of Ecology and Environment of the People's Republic
568 of China (In Chinese).
569 Gromaire-Mertz MC, Garnaud S, Gonzalez A, Chebbo G (1999) Characterisation of
570 urban runoff pollution in Paris. Water Science And Technology 39: 1-8.
571 Hale RL, Turnbull L, Earl S, Grimm N, Riha K, Michalski G, Lohse KA, Childers D
572 (2014) Sources and Transport of Nitrogen in Arid Urban Watersheds. Environmental
573 Science & Technology 48: 6211-6219.
574 HJ636-2012. (2012) Water quality-Determination of total nitrogen-Alkaline
575 potassium persulfate digestion UV spectrophotometric method.
576 HJ/T399-2007. (2007) Water quality–Determination of the chemical oxygen demand–
577 Fast digestion-spectrophotometric method. Ministry of Ecology and Environment of
578 the People's Republic of China (In Chinese).
579 Hobbie SE, Finlay JC, Janke BD, Nidzgorski DA, Millet DB, Baker LA (2017)
580 Contrasting nitrogen and phosphorus budgets in urban watersheds and implications
581 for managing urban water pollution (vol 114, pg 4177, 2017). Proceedings of the
582 National Academy of Sciences of the United States of America 114: E4116-E4116.

583 HZSB. (2020) Hangzhou Bureau of Statistics, 2020. Hangzhou Statistical Yearbook.
584 Jani J, Yang YY, Lusk MG, Toor GS (2020) Composition of nitrogen in urban
585 residential stormwater runoff: Concentrations, loads, and source characterization of
586 nitrate and organic nitrogen. Plos One 15: e0229715.
587 Janke BD, Finlay JC, Hobbie SE (2017) Trees and Streets as Drivers of Urban
588 Stormwater Nutrient Pollution. Environmental Science & Technology 51: 9569-9579.
589 Jin ZF, Qian LJ, Shi YS, Fu GW, Li GY, Li FL. 2021. Quantifying major NOx sources
590 of aerosol nitrate in Hangzhou, China, by using stable isotopes and a Bayesian isotope
591 mixing model. Atmospheric Environment 244: 117979.
592 Jin ZF, Wang Y, Qian LJ, Hu YM, Jin XP, Hong CC, Li FL (2019) Combining
593 chemical components with stable isotopes to determine nitrate sources of precipitation
594 in Hangzhou and Huzhou, SE China. Atmospheric Pollution Research 10: 386-394.
595 Kaiser J, Hastings MG, Houlton BZ, Rockmann T, Sigman DM (2007) Triple oxygen
596 isotope analysis of nitrate using the denitrifier method and thermal decomposition of
597 N2O. Analytical chemistry 79: 599-607.
598 Kaushal SS, Mayer PM, Vidon PG, Smith RM, Pennino MJ, Newcomer TA, Duan SW,
599 Welty C, Belt KT (2014) Land use and climate variability amplify carbon, nutrient,
600 and contaminant pulses: A review with management implications. Journal of the
601 American Water Resources Association 50: 585-614.
602 Kendall C, Elliott E, Wankel S (2007) Tracing Anthropogenic Inputs of Nitrogen to
603 Ecosystems. p375-449.
604 Kim LH, Ko SO, Jeong S, Yoon J (2007) Characteristics of washed-off pollutants and

605 dynamic EMCs in parking lots and bridges during a storm. Science of the Total
606 Environment 376: 178-184.
607 Kojima K, Murakami M, Yoshimizu C, Tayasu I, Nagata T, Furumai H (2011)
608 Evaluation of surface runoff and road dust as sources of nitrogen using nitrate isotopic
609 composition. Chemosphere 84: 1716-1722.
610 Kolasa-Wiecek A, Suszanowicz D. (2021) The green roofs for reduction in the load
611 on rainwater drainage in highly urbanised areas. Environmental Science and Pollution
612 Research https://doi.org/10.1007/s11356-021-12616-3
613 Krimsky LS, Lusk MG, Abeels H, Seals L (2021) Sources and concentrations of
614 nutrients in surface runoff from waterfront homes with different landscape practices.
615 Science of the Total Environment 750: 142320.
616 Lee JH, Bang KW, Ketchum LH, Choe JS, Yu MJ (2002) First flush analysis of urban
617 storm runoff. Science of the Total Environment 293: 163-175.
618 Lewis DB, Grimm NB (2007) Hierarchical regulation of nitrogen export from urban
619 catchments: Interactions of storms and landscapes. Ecological Applications 17:
620 2347-2364.
621 Li DY, Wan JQ, Ma YW, Wang Y, Huang MZ, Chen YM (2015) Stormwater Runoff
622 Pollutant Loading Distributions and Their Correlation with Rainfall and Catchment
623 Characteristics in a Rapidly Industrialized City. Plos One 10: e0118776.
624 Li LG, He ZL,, Li ZG, Zhang SH, Li SL, Wan YS, Stoffella PJ. (2016) Spatial and
625 temporal variation of nitrogen concentration and speciation in runoff and storm water
626 in the Indian River watershed, South Florida. Environmental Science and Pollution

627 Research 23: 19561-19569.
628 Li LQ, Yin CQ, He QC, Kong LL (2007a) First flush of storm runoff pollution from
629 an urban catchment in China. Journal of Environmental Sciences 19: 295-299.
630 Li MT, Chen J, Finlayson B, Chen ZY, Webber M, Barnett J, Wang M (2019a)
631 Freshwater Supply to Metropolitan Shanghai: Issues of Quality from Source to
632 Consumers. Water 11: 2176.
633 Li Q, Yu Y, Jiang XQ, Guan YT (2019b) Multifactor-based environmental risk
634 assessment for sustainable land-use planning in Shenzhen, China. Science of the Total
635 Environment 657: 1051-1063.
636 Li X, Masuda H, Koba K, Zeng H (2007b) Nitrogen Isotope Study on
637 Nitrate-Contaminated Groundwater in the Sichuan Basin, China. Water, Air, and Soil
638 Pollution 178: 145-156.
639 Liu W, Feng Q, Chen WP, C. Deo R. (2020) Stormwater runoff and pollution retention
640 performances of permeable pavements and the effects of structural factors.
641 Environmental Science and Pollution Research 27:30831-30843
642 Liu XL, Han GL, Zeng J, Liu M, Li XQ, Boeckx P (2021) Identifying the sources of
643 nitrate contamination using a combined dual isotope, chemical and Bayesian model
644 approach in a tropical agricultural river: Case study in the Mun River, Thailand.
645 Science of the Total Environment 760: 143938.
646 Lusk MG, Toor GS (2016) Biodegradability and Molecular Composition of Dissolved
647 Organic Nitrogen in Urban Stormwater Runoff and Outflow Water from a Stormwater
648 Retention Pond. Environmental Science & Technology 50: 3391-3398.

649 McIlvin MR, Casciotti KL (2011) Technical Updates to the Bacterial Method for
650 Nitrate Isotopic Analyses. Analytical chemistry 83: 1850-1856.
651 Muller A, Osterlund H, Marsalek J, Viklander M (2020) The pollution conveyed by
652 urban runoff: A review of sources. Science of the Total Environment 709: 136125.
653 Myers C, Athayde D, riscoll ED (1982) EPA's Nationwide Urban Runoff Program
654 Designed to Produce Useful Results. Civil Engineering—asce 52: 54-55.
655 Parnell AC, Inger R, Bearhop S, Jackson AL (2010) Source Partitioning Using Stable
656 Isotopes: Coping with Too Much Variation. Plos One 5: e9672.
657 Riha KM, Michalski G, Gallo EL, Lohse KA, Brooks PD, Meixner T (2014) High
658 Atmospheric Nitrate Inputs and Nitrogen Turnover in Semi-arid Urban Catchments.
659 Ecosystems 17: 1309-1325.
660 Rose LA, Elliott EM, Adams MB (2015) Triple Nitrate Isotopes Indicate Differing
661 Nitrate Source Contributions to Streams Across a Nitrogen Saturation Gradient.
662 Ecosystems 18: 1209-1223.
663 Silva CD, da Silva GBL (2020) Cumulative effect of the disconnection of impervious
664 areas within residential lots on runoff generation and temporal patterns in a small
665 urban area. Journal of Environmental Management 253: 109719.
666 Silva TFG, Vincon-Leite B, Lemaire BJ, Petrucci G, Giani A, Figueredo CC,
667 Nascimento ND (2019) Impact of Urban Stormwater Runoff on Cyanobacteria
668 Dynamics in A Tropical Urban Lake. Water 11: 946.
669 Song YL, Du XQ, Ye XY (2019) Analysis of Potential Risks Associated with Urban
670 Stormwater Quality for Managed Aquifer Recharge. International Journal of

671 Environmental Research And Public Health 16: 3121.
672 Spoelstra J, Schiff SL, Elgood RJ, Semkin RG, Jeffries DS (2001) Tracing the sources
673 of exported nitrate in the turkey lakes watershed using N-15/N-14 and O-18/O-16
674 isotopic ratios. Ecosystems 4: 536-544.
675 Sui YY, Ou Y, Yan BX, Rousseau AN, Fang YT, Geng RZ, Wang LX, Ye N (2020) A
676 dual isotopic framework for identifying nitrate sources in surface runoff in a small
677 agricultural watershed, northeast China. Journal of Cleaner Production 246: 119074.
678 Taebi A, Droste RL (2004) First flush pollution load of urban stormwater runoff.
679 Journal of Environmental Engineering and Science 3: 301-309.
680 Taylor GD, Fletcher TD, Wong THF, Breen PF, Duncan HP (2005) Nitrogen
681 composition in urban runoff - implications for stormwater management. Water
682 Research 39: 1982-1989.
683 Teaching Material Office of the Ministry of Labor and Social Security (2005) Garden
684 green space maintenance: China Labor and Social Security Publisher.
685 Toor GS, Occhipinti ML, Yang YY, Majcherek T, Haver D, Oki L (2017) Managing
686 urban runoff in residential neighborhoods: Nitrogen and phosphorus in lawn irrigation
687 driven runoff. Plos One 12: e0179151.
688 Vaze J, Chiew FHS (2004) Nutrient loads associated with different sediment sizes in
689 urban stormwater and surface pollutants. Journal of Environmental Engineering-Asce
690 130: 391-396.
691 Wang S, Feng XJ, Wang YD, Zheng ZC, Li TX, He SQ, Zhang XZ, Yu HY, Huang
692 HG, Liu T, Memon SUR, Lin CW (2019) Characteristics of nitrogen loss in sloping

693 farmland with purple soil in southwestern China during maize (Zea mays L.) growth
694 stages. Catena 182: 104169.
695 Wen HZ, Xiao Y, Wang XR, Chu LH (2019) Land-Transfer Events' Effects on the
696 Housing Market: Empirical Evidence from Hangzhou, China. Journal of Urban
697 Planning And Development 145: 04019003.
698 Widory D, Kloppmann W, Chéry L, Bonnin J, Rochdi H, Guinamant J-L (2004)
699 Nitrate in Groundwater: An Isotopic Multi-Tracer Approach. Journal of contaminant
700 hydrology 72: 165-188.
701 Wu JL, Ren YF, Wang XM, Wang XK, Chen LD, Liu GC (2015) Nitrogen and
702 phosphorus associating with different size suspended solids in roof and road runoff in
703 Beijing, China. Environmental Science And Pollution Research 22: 15788-15795.
704 Xue D, Botte J, De Baets B, Accoe F, Oertel née Nestler A, Taylor P, Cleemput O,
705 Berglund M, Boeckx P (2009) Present Limitations and Future Prospects of Stable
706 Isotope Methods for Nitrate Source Identification in Surface and Groundwater. Water
707 Research 43: 1159-1170.
708 Yan RH, Li LL, Gao JF (2019) Framework for quantifying rural NPS pollution of a
709 humid lowland catchment in Taihu Basin, Eastern China. Science of the Total
710 Environment 688: 983-993.
711 Yang H, Zhao Y, Wang JH, Xiao WH, Jarsjo J, Huang Y, Liu Y, Wu JP, Wang HJ
712 (2020) Urban closed lakes: Nutrient sources, assimilative capacity and pollutant
713 reduction under different precipitation frequencies. Science of the Total Environment
714 700: 134531.

715 Yang Y-Y, Toor G (2017) Sources and mechanisms of nitrate and orthophosphate
716 transport in urban stormwater runoff from residential catchments. Water Research 112:
717 176-184.
718 Yang YY, Lusk MG (2018) Nutrients in urban stormwater runoff: current state of the
719 science and potential mitigation options. Current Pollution Reports 4: 112-127.
720 Yang YY, Toor GS (2016) $\delta^{15}N$ and $\delta^{18}O$ reveal the sources of nitrate-nitrogen in
721 urban residential stormwater runoff. Environmental Science & Technology 50:
722 2881-2889.
723 Yue FJ, Li SL, Waldron S, Wang ZJ, Oliver DM, Chen X, Liu CQ (2020) Rainfall and
724 conduit drainage combine to accelerate nitrate loss from a karst agroecosystem:
725 Insights from stable isotope tracing and high-frequency nitrate sensing. Water
726 Research 186: 116388.
727 Zhang H, Kang X, Wang X, Zhang J, Chen G (2019) Quantitative identification of
728 nitrate sources in the surface runoff of three dominant forest types in subtropical
729 China based on Bayesian model. Science of the Total Environment 703: 135074.
730 Zhi XS, Chen L, Shen ZY (2018) Impacts of urbanization on regional nonpoint source
731 pollution: case study for Beijing, China. Environmental Science And Pollution
732 Research 25: 9849-9860.
733
734
735
736

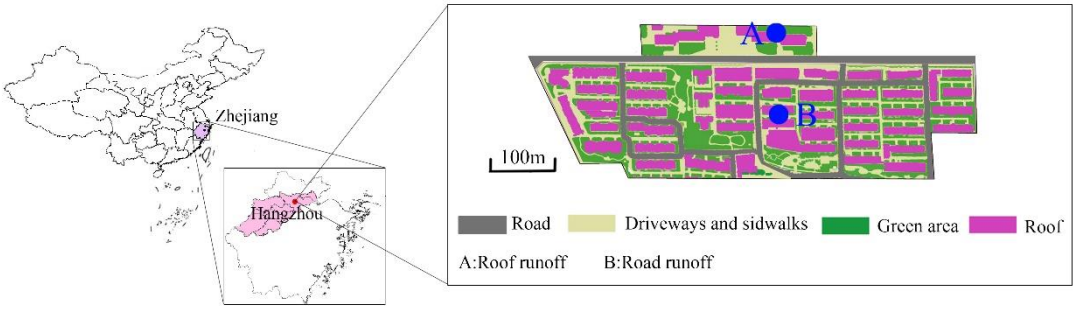

737

738 Fig. 1 Sampling sites in the study area

739

740

741

742

743

744

745

746

747

748

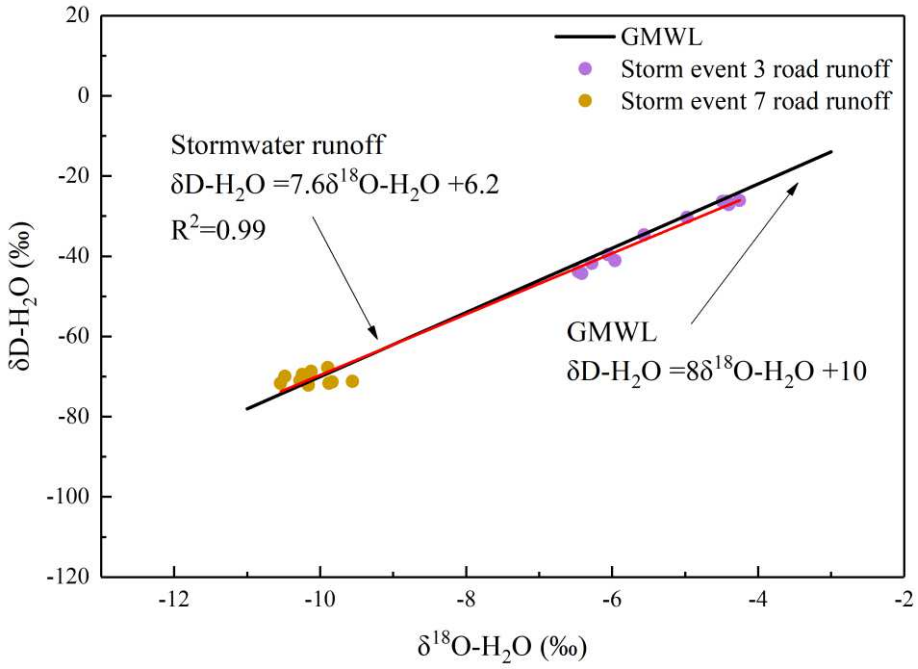

749

750 Fig. 2 Relationship between $\delta^{18}O\text{-}H_2O$ and $\delta D\text{-}H_2O$ for road runoff (n=22).

751

752

753

754

755

756

757

758

759

760

761

762

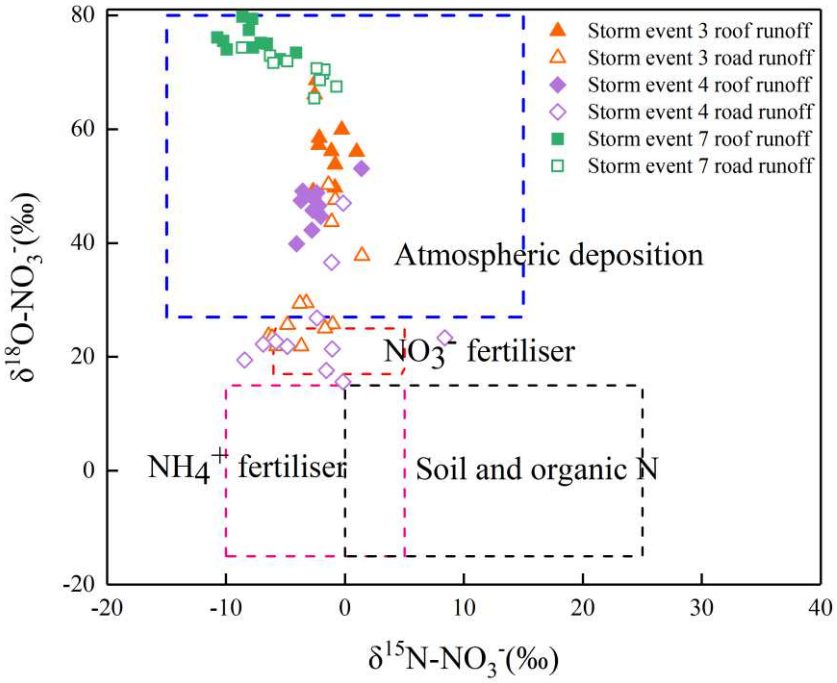

763

764 Fig. 3 $\delta^{15}N\text{-}NO_3^-$ and $\delta^{18}O\text{-}NO_3^-$ values of stormwater runoff in the urban residential

765 catchment for storm events 3, 4 and 7.

766

767

768

769

770

771

772

773

774

775

776

777

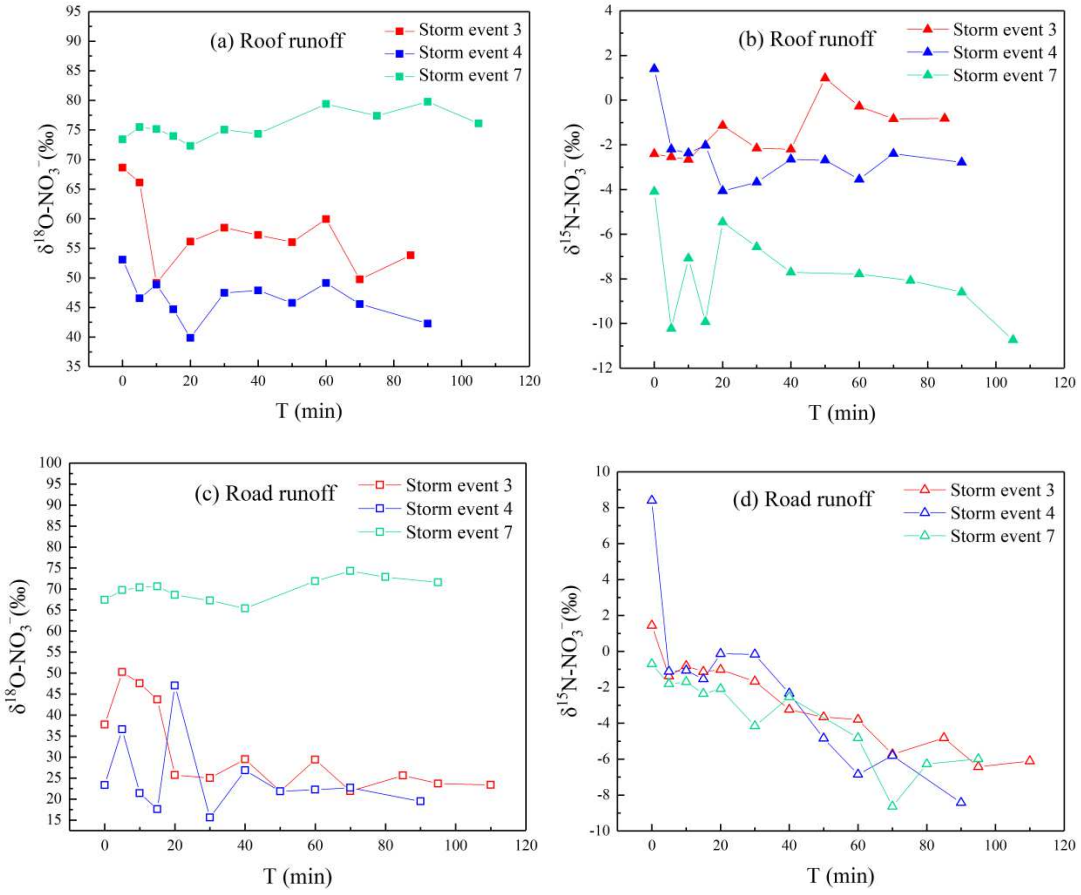

778

779 Fig. 4 Temporal variations of $\delta^{15}N\text{-}NO_3^-$ and $\delta^{18}O\text{-}NO_3^-$ in (a)–(b) roof runoff and

780 (c)–(d) road runoff.

781

782

783

784

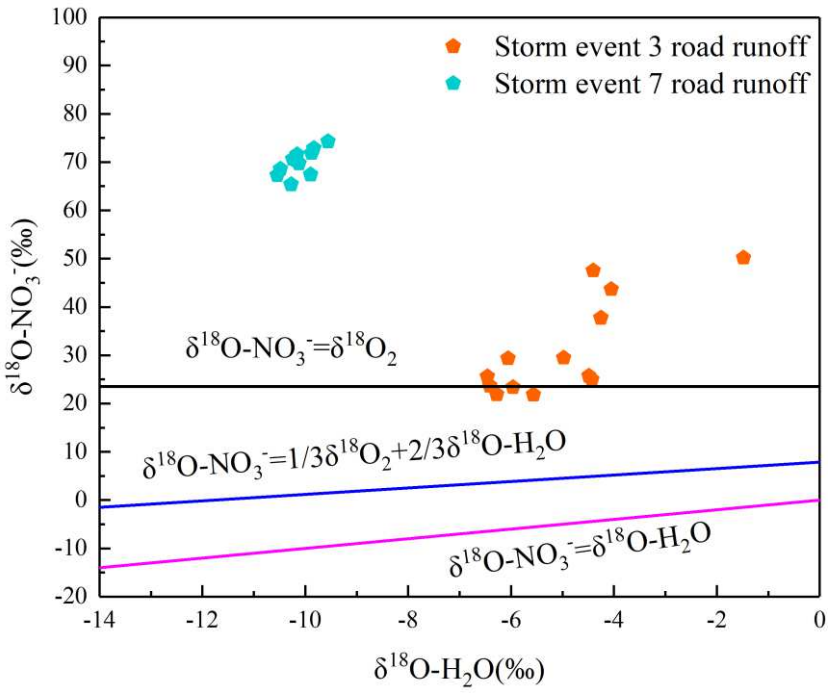

785

786 Fig. 5 Relationship between $\delta^{18}O\text{-}H_2O$ and $\delta^{18}O\text{-}NO_3^-$ in the road runoff of storm

787 events 3 and 7.

788

789

790

791

792

793

794

795

796

797

798

799

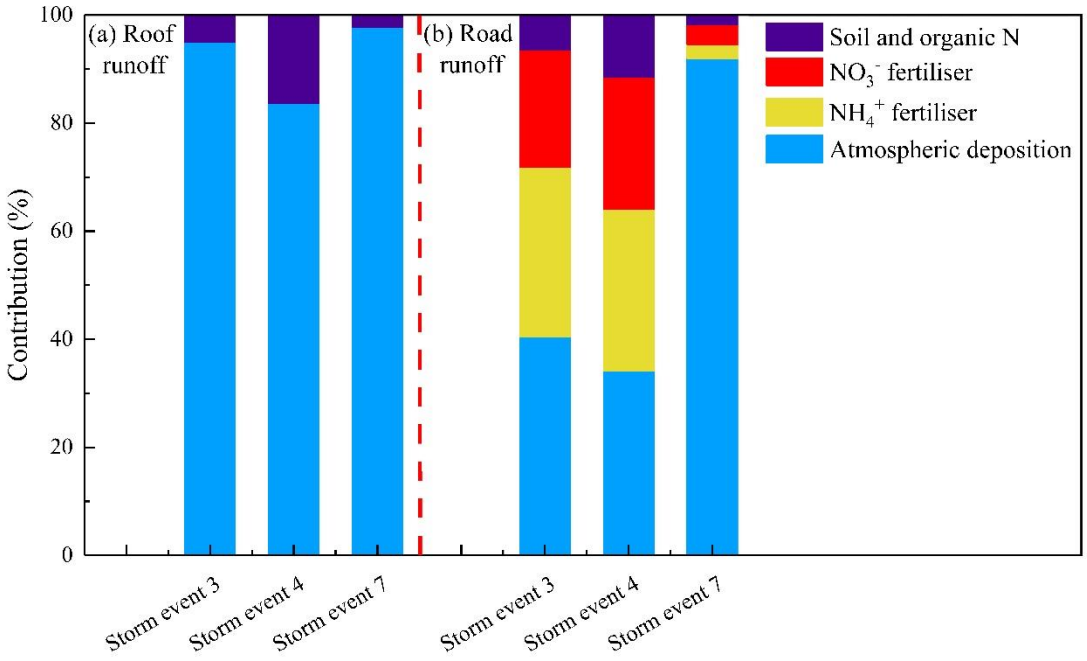

800

801 Fig. 6 Contributions of different nitrate sources in roof runoff and road runoff for

802 storm events 3, 4 and 7.

803

804

805

806

807

808

809

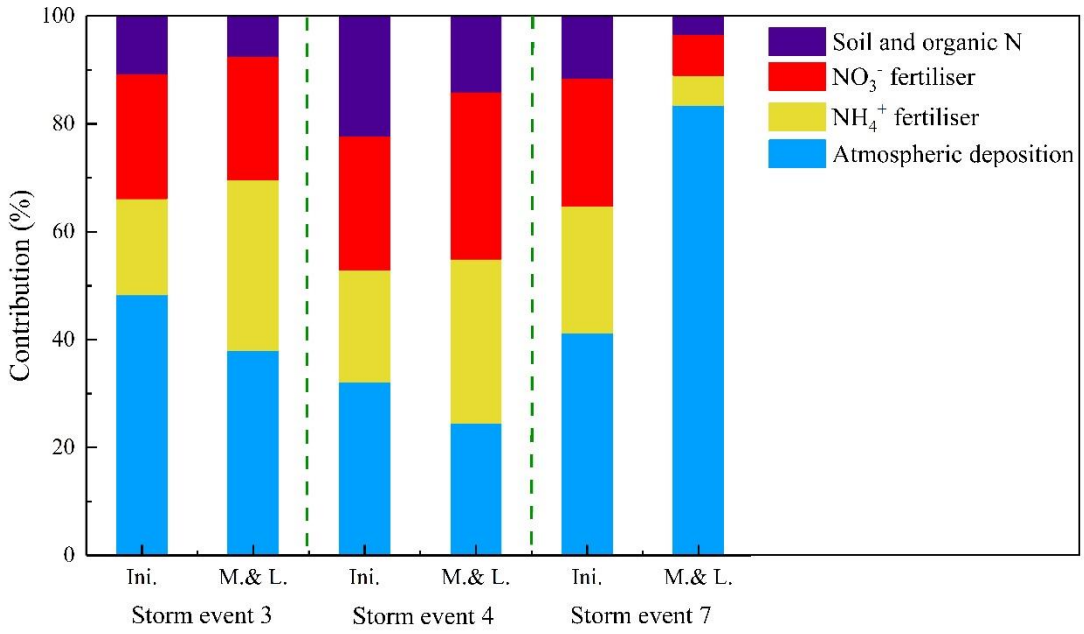

Fig. 7 Contributions of different nitrate sources in road runoff during different periods of the storm events. Ini.: initial period of stormwater runoff (first 10 minutes of sampling time); M.&L.: middle and late periods of stormwater runoff (after the first 10 minutes of sampling time)

825 Table 1 Informations on sampling of stormwater runoff in an urban residential area

826 from 2019 to 2020.

Storm event	1	2	3	4	5	6	7
Data	March 27, 2019	May 13, 2019	June 25, 2019	August 09, 2019	May 15, 2020	June 16, 2020	August 28, 2020
Antecedent dry weather period (d)	12	13	8	6	4	4	1
Rainfall intensity during sampling period (mm/h)	4.65	2.27	4.65	9.55	3.2	8.17	4
The rainfall amount during sampling period (mm)	9.3	3.4	9.3	19.1	6.4	16.3	8

827

Table 2 Statistical parameters of different N forms, TSS, COD, and the NO_3^--N/NH_4^+-N ratios in roof runoff and road runoff in an urban residential area from 2019 to 2020.

		TN mg/L	DTN mg/L	NH_4^+-N mg/L	NO_3^--N mg/L	DIN mg/L	PN mg/L	DON mg/L	TSS mg/L	COD mg/L	NO_3^--N/NH_4^+-N
roof runoff											
Storm event 1	mean	1.35	1.12	0.55	0.29	0.84	0.23	0.28	66.2	12.3	0.49
n=22	min	0.39	0.25	0.07	0.03	0.09	0.04	0.03	6	5.19	0.28
	max	3.54	3.05	1.65	1.12	2.77	0.53	0.86	114	30.4	0.85
Storm event 2	mean	2.63	2.42	0.86	0.57	1.43	0.20	0.99	45	23.7	0.61
n=23	min	0.68	0.66	0.16	0.07	0.24	0.01	0.24	2	5.56	0.22
	max	6.13	5.92	1.96	1.69	3.25	0.72	2.67	94	53.6	1.85
Storm event 3	mean	0.61	0.55	0.16	0.12	0.28	0.06	0.28	31.3	12.7	0.51
n=24	min	0.26	0.20	0.09	0.02	0.11	0.01	0.04	5	4.6	0.23
	max	2.81	2.46	0.63	1.14	1.77	0.35	0.73	92	38.6	1.81
Storm event 4	mean	0.60	0.49	0.19	0.06	0.25	0.10	0.24	47	16.1	0.29
n=24	min	0.31	0.25	0.07	BDL	0.08	0.01	0.06	12	5.61	0.00
	max	1.59	1.56	0.60	0.26	0.86	0.30	0.70	112	51.7	0.81
Storm event 5	mean	0.92	0.70	0.16	0.13	0.29	0.22	0.41	28.9	31.8	0.97
n=24	min	0.48	0.40	0.03	0.03	0.08	0.03	0.18	0	11.2	0.33
	max	1.83	1.77	0.64	0.46	1.10	0.63	0.79	78	68.1	1.91
Storm event 6	mean	1.48	1.26	0.56	0.36	0.92	0.22	0.35	33.1	24.6	0.66
n=25	min	0.33	0.21	0.13	0.08	0.21	0.01	0.00	2	5.38	0.43
	max	3.99	3.87	1.76	1.07	2.83	0.61	1.04	138	62.3	1.05
Storm event 7	mean	1.06	0.98	0.45	0.30	0.74	0.08	0.24	12.6	8.21	0.69
n=23	min	0.71	0.65	0.33	0.08	0.43	0.02	0.01	2	2.69	0.22
	max	1.56	1.46	0.72	0.47	1.19	0.17	0.59	46	18.9	1.16

road runoff											
Storm event 1	mean	3.78	1.90	0.41	0.76	1.17	1.88	0.74	142	78.2	2.04
n=25	min	0.74	0.13	0.04	BDL	0.04	0.47	0.04	8	274	0.00
	max	7.21	5.69	1.41	3.05	4.46	4.70	2.30	508	192.6	5.87
Storm event 2	mean	6.82	4.08	1.12	0.26	1.37	2.73	2.71	262.6	264.8	0.58
n=20	min	1.02	0.74	BDL	0.01	0.02	0.21	0.61	80	86.3	0.01
	max	12.70	9.69	5.28	1.64	6.04	4.81	6.56	544	412.2	3.47
Storm event 3	mean	3.87	3.12	0.71	0.95	1.66	0.76	1.46	188.8	168	1.45
n=24	min	1.99	1.68	0.28	0.41	0.88	0.04	0.25	74	52.4	0.66
	max	8.78	7.24	1.98	2.41	4.39	1.55	4.67	576	439.8	2.45
Storm event 4	mean	2.39	1.35	0.17	0.28	0.46	1.04	0.90	223	100.8	2.22
n=24	min	1.45	0.29	BDL	BDL	0.01	0.15	0.04	48	37.4	NC
	max	5.09	3.75	0.87	0.60	1.45	3.48	2.30	462	242	6.70
Storm event 5	mean	4.79	1.67	0.38	0.12	0.50	3.13	1.16	383.3	266.9	0.37
n=20	min	2.18	0.63	BDL	BDL	BDL	0.83	0.27	52	96.9	NC
	max	10.21	5.28	0.94	0.31	0.96	6.81	4.32	978	431.5	1.12
Storm event 6	mean	2.07	1.37	0.48	0.29	0.77	0.70	0.60	198.4	86.1	1.60
n=20	min	0.65	0.40	0.01	BDL	0.15	0.21	0.25	80	34.7	0.00
	max	4.48	3.47	1.54	1.22	2.77	2.13	1.50	484	217.8	9.15
Storm event 7	mean	2.95	1.67	0.34	0.66	1.00	1.28	0.67	138	83.7	2.33
n=23	min	1.10	0.71	0.11	0.21	0.32	0.04	0.39	4	8.08	0.75
	max	6.61	2.82	0.66	1.48	2.08	3.94	1.10	444	253.5	4.00

n: Number of the samples

BDL: below the detection limit;

NC: When the NH_4^+-N concentrations were below the detection limit, the NO_3^--N/NH_4^+-N ratios were not calculated.

Supplementary Files

This is a list of supplementary files associated with this preprint. Click to download.

- 1DataESPR.docx
- 1suplimentaryESPR.docx